THE JOURNAL OF BIOLOGICAL CHEMISTRY VOL. 292, NO. 7, pp. 3049–3059, February 17, 2017

GMP Synthase Is Required for Virulence Factor Production and Infection by *Cryptococcus neoformans*[*][S]

Received for publication, November 11, 2016, and in revised form, January 4, 2017 Published, JBC Papers in Press, January 6, 2017, DOI 10.1074/jbc.M116.767533

Jessica L. Chitty[‡§], Tayla L. Tatzenko[‡], Simon J. Williams[‡¶], Y. Q. Andre E. Koh[‡], Elizabeth C. Corfield[‡], Mark S. Butler[§], Avril A. B. Robertson[§], Matthew A. Cooper[‡§], Ulrike Kappler[‡‖], Bostjan Kobe[‡§], and James A. Fraser[‡1]

From the [‡]Australian Infectious Diseases Research Centre, School of Chemistry & Molecular Biosciences, the [§]Institute for Molecular Bioscience, and the [‖]Centre for Metals in Biology, University of Queensland, St. Lucia, Queensland 4072, Australia and the [¶]ANU Research School of Biology, Australian National University, Acton, ACT 2601, Australia

Edited by John M. Denu

Over the last four decades the HIV pandemic and advances in medical treatments that also cause immunosuppression have produced an ever-growing cohort of individuals susceptible to opportunistic pathogens. Of these, AIDS patients are particularly vulnerable to infection by the encapsulated yeast *Cryptococcus neoformans*. Most commonly found in the environment in purine-rich bird guano, *C. neoformans* experiences a drastic change in nutrient availability during host infection, ultimately disseminating to colonize the purine-poor central nervous system. Investigating the consequences of this challenge, we have characterized *C. neoformans* GMP synthase, the second enzyme in the guanylate branch of *de novo* purine biosynthesis. We show that in the absence of GMP synthase, *C. neoformans* becomes a guanine auxotroph, the production of key virulence factors is compromised, and the ability to infect nematodes and mice is abolished. Activity assays performed using recombinant protein unveiled differences in substrate binding between the *C. neoformans* and human enzymes, with structural insights into these kinetic differences acquired via homology modeling. Collectively, these data highlight the potential of GMP synthase to be exploited in the development of new therapeutic agents for the treatment of disseminated, life-threatening fungal infections.

In the past four decades there has been a dramatic escalation in the number of immunocompromised individuals (1). Although many of these are due to advances in immunosuppressive and chemotherapeutic technologies, the largest cohort is a direct result of the AIDS pandemic. Foreshadowed in 1981 with the occurrence of opportunistic *Pneumocystis* or human herpesvirus 8 infections in previously healthy individuals in Los Angeles (2, 3), AIDS and the lentivirus causing the disease soon gained broad public awareness (4–6). With the advent of commercial blood testing, national blood bank screening programs were commenced in an effort to slow the spread of this emerging pandemic (7), and in 1987 the first treatment, zidovudine, marked what was thought to be an end to the crisis (8, 9). It was not, as was hoped, a miracle drug; the spread of AIDS continued across the globe and is now believed to have infected over 70 million people and killed 55 million to date (10).

Since the discovery of the very first patients identified with *Pneumocystis* pneumonia, opportunistic fungal pathogens have been tightly linked with the AIDS pandemic. One of the key fungi often encountered in this context is *Cryptococcus neoformans*, a basidiomycete yeast responsible for cryptococcosis and a major cause of AIDS-related mortality (11). Most commonly found associated with purine-rich bird guano, spores or desiccated yeast cells from this environmental niche are inhaled into the lungs where, in an immunocompromised individual, the fungus can disseminate to the purine-poor central nervous system to cause meningoencephalitis.

The fundamental treatment for cryptococcosis has not changed significantly in over two decades and consists of induction with amphotericin B and flucytosine followed by consolidation and maintenance phases employing fluconazole (12–16). Each of these therapeutic agents exploit an aspect of fungal physiology that differs from the human host: the presence of ergosterol rather than cholesterol in the cell membrane, the existence of the pyrimidine salvage enzyme cytosine deaminase, or changes in the sterol biosynthetic pathway, respectively. Even so, each of these agents still cause side effects, epitomized by the compromised renal function typical of amphotericin B use.

The similarity in physiology between human host and fungal pathogen means there are few gross differences that can be easily targeted via rational drug design. However, differences such as slight changes in the active site of enzymes in a highly conserved essential pathway may be exploited, as typified by fluconazole. One such potential target is *de novo* purine biosynthesis, the pathway in which the process of rational drug design was pioneered (17–19). Proliferating cells require vast quantities of ATP and GTP to meet the demands of replication, transcription, and energy metabolism. Purine biosynthesis is therefore essential in rapidly dividing immune cells, cancers, or

* This work was supported by National Health and Medical Research Council Grant APP1049716 (to J. A. F. and M. S. B.), a Queensland Medical Research Scholarship (to J. C.), National Health and Medical Research Council Principle Research Fellowships 1003325 and 1110971 (to B. K.), and National Health and Medical Research Council Principle Research Fellowship GNT1059354 (to M. A. C.). The authors declare that they have no conflicts of interest with the contents of this article.

[S] This article contains supplemental Tables S1 and Figs. S1 and S2.

[1] To whom correspondence should be addressed: Australian Infectious Diseases Research Centre, School of Chemistry & Molecular Biosciences, University of Queensland, St. Lucia, QLD 4072 Australia. E-mail: jafraser@uq.edu.au.

infecting microbes. The pathway is already a target for anticancer drugs (such as mercaptopurine and lometrexol) and immunosuppressants (such as mycophenolic acid) (20–24). However, the investigation of purine metabolism as an antifungal target has been limited (25–27).

Purine metabolism is of particular interest in *C. neoformans* because of the gross disparity in purine concentrations in bird guano compared with the central nervous system of the infected human host (28–30). The importance of *de novo* biosynthesis rather than scavenging while the fungus infects this purine-poor environment was highlighted by the discovery that IMP dehydrogenase, catalyst of the rate-limiting and first committed step in the *de novo* GTP biosynthesis pathway, is essential for *C. neoformans* virulence in a murine model. Importantly, structural studies of this enzyme revealed potentially exploitable characteristics of the fungal enzyme not shared with the human isoforms (25).

IMP dehydrogenase is not the only enzyme in *de novo* GTP biosynthesis that has potential as an antimycotic target. Following IMP dehydrogenase in the guanylate branch of *de novo* purine biosynthesis is GMP synthase (E.C. 6.3.5.2). Originally identified in ground rabbit bone marrow (31) and pigeon liver (32), the key work that underpins our current understanding of GMP synthase was performed in *Escherichia coli* (33, 34), and this system continues to be the source for a detailed biochemical understanding of the activity of the enzyme (35–37).

GMP synthase is a monofunctional enzyme in all organisms studied so far, with two catalytic modules working in concert to ensure efficient amination of xanthine monophosphate (XMP)[2] to GMP. The magnesium-dependent ATP pyrophosphatase (ATP-PPase) domain reversibly adenylates XMP to form a covalent O^2-adenyl-XMP intermediate; this activates the C^2 carbon of XMP for attack by the amide side chain of glutamine, liberated by the class I glutamine amidotransferase (GATase) domain (33, 34, 38).

Crystal structure determination of *E. coli* GMP synthase identified the enzyme as having three distinct domains: the N-terminal ATP-PPase domain, the GATase domain, and a C-terminal dimerization domain, and supported early sedimentation velocity experiments indicating *E. coli* GMP synthase forms a homodimer (34, 39). GMP synthase structures are now available for other bacterium (*Coxiella burnetii* (40) and *Thermus thermophiles* (PDB codes 2YWB and 2YWC)), archaea (*Pyrococcus horikoshii* (41)), and two eukaryotes (*Plasmodium falciparum* (42), *Homo sapiens* (43)); all contain ATP-PPase, GATase, and dimerization domains.

In contrast, few studies of GMP synthase have been performed in fungi. The GMP synthase gene has been identified and mutated in *Saccharomyces cerevisiae*, *Candida albicans*, and *Aspergillus fumigatus*; as expected, these mutants were all guanine auxotrophs (26, 44–46). Furthermore, the GMP synthase mutants of *C. albicans* and *A. fumigatus* were avirulent in murine infection models (26). No kinetics or structural studies of fungal GMP synthases are available.

Here, we describe the characterization of GMP synthase from *C. neoformans*, showing the potential of the enzyme as a broad spectrum antifungal target. Using genetic techniques, we demonstrate that GMP synthase is required for *C. neoformans* virulence factor production and successful infection of the host. With the aid of biochemical analyses and structural modeling, we identify key functional differences between GMP synthase from *C. neoformans* and humans, thereby delineating its suitability as a potential antifungal drug target.

Results

Identification of the GMP Synthase-encoding Gene in C. neoformans—To begin our characterization of GMP synthase from *C. neoformans*, the corresponding gene in the type strain H99 genome was identified via a reciprocal best hit BLAST analysis employing the *S. cerevisiae* ortholog *GUA1* (45). A single hit was observed, indicating that the gene is present in single copy. Located on chromosome 11, this locus was designated as *CNAG_018770* in the published H99 genome (47); subsequently employing *CNAG_018770* as the query sequence in a BLAST search of the *S. cerevisiae* genome identified *GUA1* as the only hit in that species. The gene *CNAG_018770* has therefore been named *GUA1* after the *S. cerevisiae* ortholog, whose predicted product is 65% identical at the amino acid level. In comparison, Gua1 is 50% identical to GuaA in *E. coli*, 35% identical to human GuaA isoform 1, 23% identical to the human GuaA, and 23% identical to human GuaA isoform 2.

Gua1 Is Essential for Guanine Protrophy in C. neoformans—To verify that the identified gene designated as *GUA1* encodes GMP synthase, we performed a biolistic targeted gene deletion in *C. neoformans* type strain H99. Consistent with our bioinformatic predictions, the *gua1*Δ strain could not grow on YNB minimal medium, but growth was restored (albeit incompletely) upon the addition of guanine (Fig. 1*B*). The *gua1*Δ strain was not, however, able to utilize the guanine naturally present in rich YPD medium, nor was growth restored by the addition of exogenous guanine to YPD (data not shown); this unusual phenotype was consistent with that previously reported for the IMP dehydrogenase *imd1*Δ mutant (25). Reintroducing a wild-type copy of the gene to create strain *gua1*Δ+*GUA1* restored growth on both YNB and YPD medium (Fig. 1*B*). Together, these data are consistent with *GUA1* encoding GMP synthase.

To gain insight into potential growth defects that may be exhibited during infection independent of guanine starvation, the effect of deleting *GUA1* on the growth rate was investigated in RPMI 1640 medium supplemented with 1 mM guanine. Again, even in the presence of guanine, the *gua1*Δ mutant displayed slower growth compared with both wild type and the complemented *gua1*Δ+*GUA1* strain because of an extended lag phase (Fig. 1*C*). Furthermore, the mutant reached stationary phase at an optical density lower than the wild-type or complemented strains. The delayed and reduced growth of the mutant, even in the presence of guanine concentrations far exceeding the limited amounts in mammalian cerebrospinal fluid (~0.5

[2] The abbreviations used are: XMP, xanthine monophosphate; PDB, Protein Data Bank; GATase, glutamine amidotransferase; DON, 6-diazo-5-oxo-L-norleucine; SEC, size exclusion chromatography; MALLS, multiangle laser light scattering; LB, lysogeny broth; NGM, nematode growth medium; BHI, brain-heart infusion; L-DOPA, L-3,4-dihydroxyphenylalanine; AMP-PNP, adenosine 5′-(β,γ-iminotriphosphate).

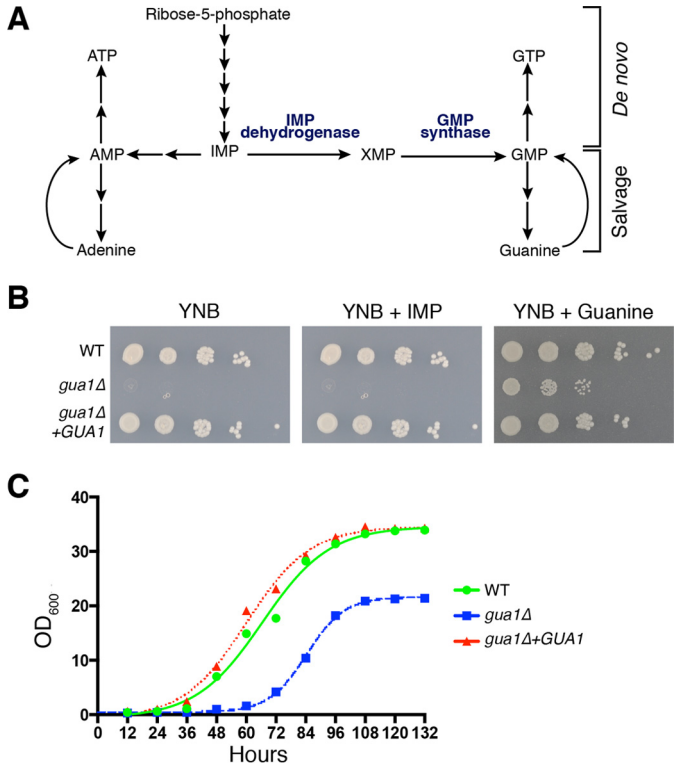

FIGURE 1. **The *de novo* and salvage purine biosynthesis pathway and GMP synthase role in GTP biosynthesis.** *A*, IMP dehydrogenase and GMP synthase catalyze the first two steps of the guanylate branch of *de novo* purine biosynthesis. *B*, 10-fold serial dilutions of indicated strains were spotted onto YNB medium supplemented with specified purines (1 mM) and incubated for 2 days at 30 °C. *C*, strains were grown for 6 days in RPMI 1640 medium supplemented with 10% serum and 1 mM guanine at 30 °C, with A_{600} readings collected every 12 h.

μM (29)), suggested the mutant was likely to exhibit severe attenuation or avirulence in infection models.

Loss of GMP Synthase Affects Production of C. neoformans Virulence Determinants—During the infection process, *C. neoformans* relies on a number of key virulence factors that play an important role in protecting the pathogen from host defenses, facilitating dissemination and growth. To observe the effects of the *gua1*Δ mutation on the production of these virulence factors while limiting the confounding influence of guanine starvation influencing growth, *in vitro* virulence factor production assays were performed in the presence of exogenous guanine. The complex polysaccharide capsule protects the fungal cells against phagocytosis by immune cells during infection. When grown in guanine-supplemented capsule-inducing RPMI 1640 medium, the *gua1*Δ mutant produced significantly less capsule than wild type and the complemented *gua1*Δ+*GUA1* strain after 30 h at both 30 and 37 °C ($p < 0.0001$; Fig. 2*A*). The virulence factor melanin protects *C. neoformans* against the effects of oxidants, such as those produced by phagocytic cells. When plated on guanine-supplemented L-3,4-dihydroxyphenylalanine (L-DOPA) medium, production of melanin was delayed; this delay was more pronounced at 37 °C. Production of proteases enables *C. neoformans* to degrade host tissue and facilitate dissemination, as well as obtain nutrients for growth. On guanine-supplemented protease-inducing medium, protease activity was undetectable in the *gua1*Δ mutant at either 30 or 37 °C (Fig. 2). In summary, loss of GMP synthase was associated with delayed or abolished production of the known virulence factors capsule, melanin, and proteases, and this was more pronounced at human body temperature, providing further evidence that the *gua1*Δ mutant was likely to exhibit impaired virulence.

GMP Synthase Is Critical for C. neoformans Virulence in Both Nematode and Murine Models—The compromised growth rate and virulence factor production of the *gua1*Δ mutant strongly suggested the strain would be unlikely to successfully cause infection. Evaluation of virulence was first performed in the nematode *Caenorhabditis elegans*, a natural predator of *C. neoformans* (64). Nematodes were introduced onto a lawn of wild-type, *gua1*Δ, or *gua1*Δ+*GUA1* cells grown on rich brain-heart infusion (BHI) medium, minimal nematode growth medium (NGM), and minimal NGM supplemented with 1 mM guanine. No difference in virulence was observed between the wild-type, *gua1*Δ, and *gua1*Δ+*GUA1* strains when grown on BHI or NGM supplemented with guanine ($p > 0.1$; Fig. 3*A*). Given the abundance of guanine in bird guano, this result was consistent with what could be expected in the environmental niche where *C. neoformans* encounters this predator. However, on NGM lacking guanine supplementation, the *gua1*Δ mutant was avirulent ($p < 0.0001$; Fig. 3*A*).

The nematode data indicated the importance of GMP synthase for virulence was influenced by the abundance of guanine available. Given the low concentrations of available purines in cerebrospinal fluid (28–30), we investigated the effect of *gua1*Δ on virulence using a murine inhalation model of cryptococcosis. Mice infected with the wild-type and *gua1*Δ+*GUA1* strains displayed equivalent progression of disease, succumbing to the infection within 20 days (Fig. 3*B*). In contrast, rather than losing weight and displaying other disease-associated symptoms, all mice infected with the *gua1*Δ strain gained weight and were healthy until the 60-day end point of the experiment (Fig. 3*B*). Furthermore, fungal burden analysis from sacrificed animals showed the infection had been cleared from all mice infected with the *gua1*Δ mutant, similar to previous observations (25).

C. neoformans GMP Synthase Enzyme Kinetics Show Differences to the Human Ortholog in Binding Cooperativity—Given the importance of Gua1 during murine infection, we expanded our analyses to investigate the biochemical function of *C. neoformans* GMP synthase. To identify possible functional differences between the fungal and human enzymes that could be exploited in therapeutic agent development, His-tagged *C. neoformans* Gua1 was expressed in *E. coli* and purified, and the histidine tag was removed prior to use of recombinant Gua1 in steady-state kinetic analysis.

The dual catalytic action of GMP synthase is required for the amination of XMP to GMP and involves two main steps: initially adenyl-XMP is produced by the ATP pyrophosphatase (ATP-PPase) domain in the presence of Mg^{2+}, and this product then reacts with ammonia produced by the hydrolysis of glutamine that is catalyzed by the N-terminal glutamine amidotransferase (GATase) (33, 38). The amination of XMP in *C. neoformans* GMP synthase protein displayed Michaelis-Menten kinetics with a K_m of 65.9 ± 13.0 μM and a k_{cat} of 0.4 s^{-1} for the overall reaction. ATP adenylation also exhibited Michaelis-

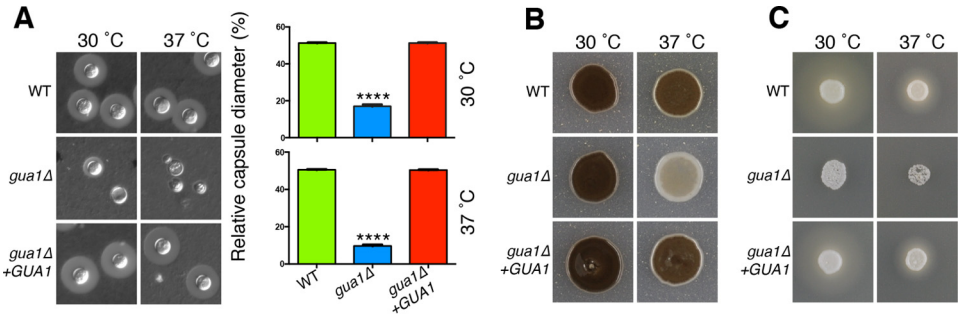

FIGURE 2. **Loss of *GUA1* compromises virulence factor production.** *A*, *C. neoformans* strains were incubated in RPMI 1640 medium, 10% fetal bovine serum, and 1 mM guanine at 30 and 37 °C. At 30 h, the cells were stained with India ink. The relative capsule diameter value shows the mean, and the *error bars* represent S.E. ****, $p < 0.0001$. *B*, melanin production was determined on L-DOPA medium with strains incubated at 30 and 37 °C for 48 h. *C*, protease production was determined on YNB medium with amino acids and 0.1% bovine serum albumin plates with strains at 30 and 37 °C for 48 h.

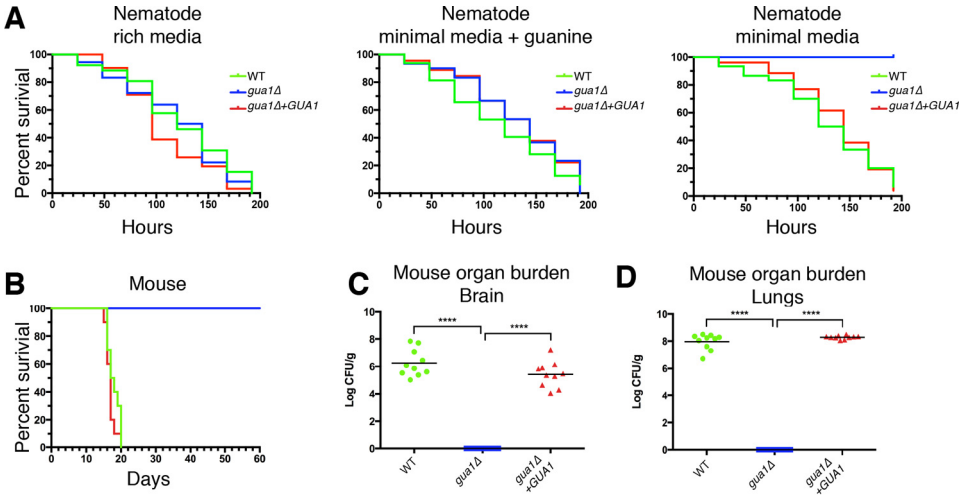

FIGURE 3. **Virulence of *gua1*Δ mutant in nematode and murine host systems.** *A*, Bristol N2 *C. elegans* were transferred onto lawns of the indicated *C. neoformans* strains grown on BHI medium, minimal medium, and minimal medium supplemented with 1 mM guanine and incubated at 28 °C, and survival was monitored. For minimal medium, the *gua1*Δ mutant strain was avirulent, differing from the wild-type or *gua1*Δ+*GUA1* strains ($p < 0.0001$). No significant difference in virulence was found between strains when grown on rich medium or minimal medium supplemented with guanine ($p > 0.1$). *B*, virulence of the *gua1*Δ mutant in the murine inhalation model of infection. 6-week-old female BALB/c mice were infected with H99, *gua1*Δ, or *gua1*Δ+*GUA1 C. neoformans* strains ($n = 10$), and survival was monitored over 60 days. Survival of mice with wild-type or *gua1*Δ+*GUA1* strains showed no significant difference ($p > 0.05$), and survival was significantly lower than in those infected with the avirulent *gua1*Δ mutant strain ($p < 0.0001$). *C* and *D*, posthumous organ burden was calculated in colony-forming units (CFU)/g of organ as described.

Menten kinetics and had a K_m of 77.5 ± 6.0 μM. In contrast, kinetic data for Mg^{2+}, which is required as a co-factor for the reaction of XMP to adenyl-XMP, revealed a sigmoidal response to increases in substrate concentration, which is indicative of cooperative binding and was best fitted with a Hill coefficient (n) of 2.2 ± 0.2 and a $K_{0.5}$ of 1289.0 ± 66.0 μM. The final part of the reaction, hydrolysis of glutamine by the GATase domain in the *C. neoformans* protein, displayed Michaelis-Menten kinetics and had a K_m of 1130.0 ± 162.0 μM, showing a low affinity for this substrate.

Compared with previously identified GMP synthases, the kinetic parameters of the *C. neoformans* enzyme were most similar to those of the *Mycobacterium tuberculosis* GMP synthase, which was reported to have similar binding affinity. For XMP, the binding affinity was only moderately lower between *C. neoformans* (65.9 ± 13.0 μM) and *M. tuberculosis* (45.0 ± 1.0 μM) and different between human (35.6 ± 1.8 μM) and *C. neoformans*, and unlike *M. tuberculosis* and human enzymes, the *C. neoformans* enzyme did not show cooperative binding of XMP (58, 59). The K_m of ATP is moderately higher than reported in *M. tuberculosis* (27 ± 2 μM) but considerably lower than human GMP synthase (132 ± 7 μM). The affinity for glutamine and Mg^{2+} in *C. neoformans* GMP synthase was most like *M. tuberculosis* (Table 1). However, the magnitude of the positive cooperativity observed for XMP binding in the human enzyme was moderate, with a Hill (n) coefficient of 1.48 (59), whereas *M. tuberculosis* GMP synthase had a Hill (n) coefficient of 2.4 (58). Overall, the human GMP synthase protein had a significantly higher (~12×) turnover number than the *C. neoformans* protein, and the concentration of glutamine required to reach saturation was almost three times higher for *C. neoformans* (1130 ± 162 μM) compared with human GMP synthase enzyme (406 ± 49 μM) (58, 59), confirming potentially important kinetic differences in these enzymes.

ECC1385 Is an Inhibitor of C. neoformans GMP Synthase—Given the biochemical differences uncovered above and the importance of GMP synthase in virulence in *C. neoformans*, we next investigated the ability to phenocopy the *gua1*Δ phenotype with a chemical inhibitor. The best known inhibitor of GMP synthase is 6-diazo-5-oxo-L-norleucine (DON), a well characterized glutamine agonist that targets several glutamine binding proteins, in particular phosphoribosylformylgly-

TABLE 1

Comparison of kinetic parameters of GMP synthase from different organisms

The values are shown ± S.E. ND denotes no data. The assay conditions used were as follows: *C. neoformans* (Tris buffer, pH 7.5, 0.15 mM XMP, 1 mM ATP, 5 mM glutamine, and 20 mM $MgCl_2$), *E. coli* (60 mM Hepes buffer, pH 8, 0.2 mM XMP, 5 mM ATP, 200 mM glutamine, 20 mM $MgCl_2$), *M. tuberculosis* (50 mM Tris buffer, pH 7.5, 0.15 mM XMP, 1 mM ATP, 5 mM glutamine, 20 mM $MgCl_2$), *P. falciparum* (90 mM Tris buffer, pH 8.5, 0.15 mM XMP, 2 mM ATP, 5 mM glutamine, 20 mM $MgCl_2$), and *H. sapiens* (75 mM Tris buffer, pH 7.8, 1 mM XMP, 2 mM ATP, 5 mM glutamine, 10 mM $MgCl_2$).

Species	$K_{cat(XMP)}$	$K_{m(XMP)}$	n	$K_{m(ATP)}$	$K_{m(Gln)}$	$K_{0.5(Mg^{2+})}$	Reference
	s^{-1}	μM		μM	μM	μM	
C. neoformans	0.41	65.9 ± 13	ND	77.5 ± 6	1130 ± 162	1289 ± 66	This work
E. coli	ND	166 ± 43	ND	104 ± 44	ND	ND	Ref. 35
M. tuberculosis	2.3	45 ± 1[a]	2.4	27 ± 2	1240 ± 60	1180 ± 30	Ref. 58
P. falciparum	0.43	16.8 ± 2	ND	260 ± 38	472 ± 69	2090 ± 30	Ref. 71
H. sapiens[b]	5.4	35.6 ± 1.8[a]	1.48	132 ± 7	406 ± 49	1780 ± 70	Ref. 59

[a] $K_{0.5}$ (for substrates where cooperativity was observed) instead of K_m.
[b] A second variant for humans has been reported, but values between the two were catalytically indistinguishable.

cinamidine synthetase and CTP synthetase (65–67). In the context of antimycotic development, however, a nonspecific inhibitor is of little interest because a number of off target effects in the host would be anticipated, and so it was deemed unsuitable for this study. Ones potentially important lead compound was ECC1385, a synthetic compound that showed potent activity against a number of other fungal pathogens (26). A genetics-based investigation revealed that ECC1385 had potency against the GMP synthases from *C. albicans* and *A. fumigatus* and that the compound had a different mode of action to a glutamine agonist (26).

We tested ECC1385 as a direct inhibitor of purified *C. neoformans* GMP synthase using concentrations between 0 and 200 μM, which revealed an IC_{50} of 4.4 μM, providing the first biochemical evidence that ECC1385 acts directly on the activity of purified GMP synthase. However, subsequent broth dilution assays to determine the inhibitory action of ECC1385 against *C. neoformans* failed to inhibit growth, despite employing a concentration range reaching 100 μM, far exceeding the potency determined in the enzyme assay. Importantly, although this compound cannot serve as an antifungal itself, it provides evidence that the activity of GMP synthase can be inhibited without depending on a nonspecific agent.

Predicted Differences between Human and C. neoformans GMP Synthase—The process of rational drug design can be greatly facilitated by the knowledge of the three-dimensional structure of the target. To this end, we endeavored to solve the crystal structure of *C. neoformans* GMP synthase; however, despite extensive efforts, we were unable to obtain a protein structure because of poor crystal quality.

To gain insight into GMP synthase structure in the absence of a crystal structure, we used size exclusion chromatography (SEC) coupled with multiangle laser light scattering (MALLS) to determine the oligomeric state of GMP synthase in solution. Human GMP synthase is a monomer in solution with a small dimer population; however, in the active form, when all substrates are bound, there is evidence that it forms a dimer (43). In contrast, *E. coli* GMP synthase is a homodimer is solution (39, 68). The elution profile for *C. neoformans* GMP synthase demonstrates that this protein predominantly forms a dimer (120 kDa) in solution, with a small tetramer population (Fig. 4). The quaternary structure of *C. neoformans* GMP synthase is therefore more similar to *E. coli* than the human protein.

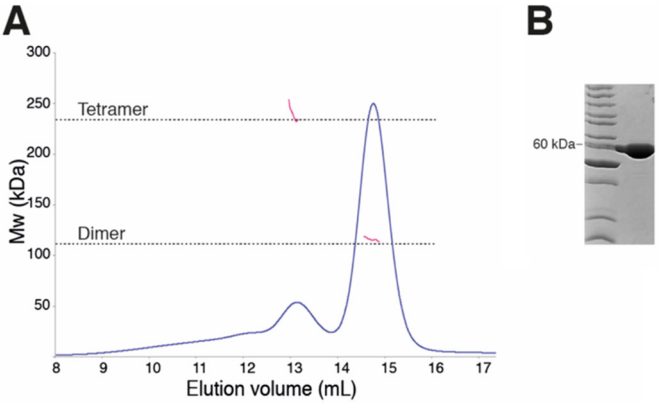

FIGURE 4. **Solution properties of *C. neoformans* Gua1.** *A*, *blue lines* indicate the trace from the refractive index detector (arbitrary units) during size exclusion chromatography. *Magenta lines* indicate the average molecular weight (*y* axis) distribution across the peak by MALLS. *B*, SDS-PAGE confirms the mass of a monomer of GMP synthase at ~60 kDa.

To compare potential structural differences between the human and *C. neoformans* enzymes, a homology model (63) of *C. neoformans* GMP synthase was generated using the *E. coli* enzyme as a template; there are no reported fungal GTP synthase structures, and of those species for which a structure has been determined, the *E. coli* enzyme exhibited the highest protein identity (50%) with *C. neoformans* (34).

Overall, the structural model of *C. neoformans*, based on the *E. coli* structure, has three distinct regions: dimerization, ATP-PPase, and GATase domains (Fig. 5). The human GMP synthase has been reported to have two distinct groups of its dimerization domain (D1 and D2) as well as the ATP-PPAse and GATase domains, and in this respect *C. neoformans* GMP synthase is more closely related to *E. coli* (Fig. 5). Like *E. coli*, *C. neoformans* GMP synthase is a dimer in solution (Fig. 4), whereas human GMP synthase is a monomer in solution and believed to dimerize upon substrate binding.

Although lacking two subsections, the dimerization domain of *E. coli* and *C. neoformans* includes most amino acids required for XMP binding, and the highly conserved dimerization subdomain with the consensus sequence Val-Gly-Val-Xaa-Gly-Asp-Xaa-Arg-Xaa-Tyr (supplemental Fig. S3). This subdomain is present in the D1 domain of human GMP synthase rather than D2, which has a high level of identity with *C. neoformans* and *E. coli* GMP synthase.

In the human GATase domain, three key residues are involved in the binding of glutamine: Cys^{104}, His^{190}, and

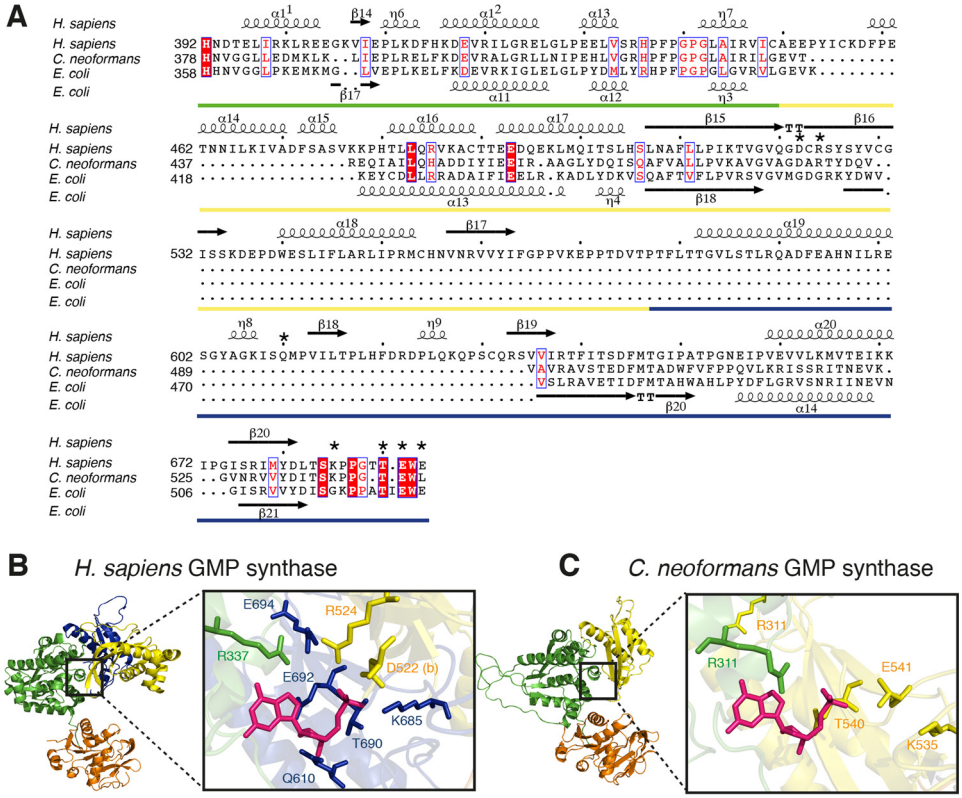

FIGURE 5. **Comparison of GMP synthase from human and *C. neoformans* in complex with XMP.** *A*, sequence alignment of human and *C. neoformans* GMP synthases prepared using the server ESPript (72). *Fuchsia* represents XMP, *orange* represents the GATase domain, *green* represents the ATP-PPase domain, *blue* represents the D1 domain, and *yellow* represents the D2 (human) or dimerization domain (*C. neoformans*). *Asterisks* highlight residues involved in XMP binding. *B*, the structure of human GMP synthase (PDB code 2VXO), colored as for *A*. The amino acids responsible for XMP binding are identified as *sticks*. Asp^{522} is contributed by the second monomer. *C*, the structural model of *C. neoformans* GMP synthase was modeled based on the ortholog from *E. coli*. When compared with the human GMP synthase, *C. neoformans* does not have Gln^{610} and shows a single amino acid change at position Leu^{544}, compared with Glu^{694} in the human enzyme.

Glu^{192}. These residues form a catalytic triad that is highly conserved among the amidotransferases, and it is also conserved in *C. neoformans* GMP synthase (supplemental Fig. S3), as well as *E. coli* (data not shown) (43). The XMP binding site would be a more viable drug target of GMP synthase given that glutamate analogs, such as DON, target other enzymes as well. Of the residues that interact with XMP in human GMP synthase, one residue, Gln^{610}, was particularly interesting because it is part of the D1 domain that is absent from *C. neoformans* GMP synthase (43). Two other residues were not identified in the model but can be seen in the sequence alignment as being conserved. Given the large conformation change believed to occur during XMP amination and the homology model based on AMP-bound *E. coli* GMP synthase, the model may not represent the XMP-bound state. The D2 domain contains other amino acids, which contribute to XMP binding, and for the most part, these amino acids are conserved; however, at position Glu^{694} in the humans enzyme, *C. neoformans* GMP synthase has a leucine.

Discussion

C. neoformans GMP synthase was identified based on similarity to the *S. cerevisiae* ortholog *GUA1*. The mutant phenotype following deletion by biolistic transformation showed that the enzyme is essential for fungal growth on minimal medium and required for multiple phenotypes associated with virulence. These virulence factors are key to *C. neoformans* survival in the human host; defects in production of melanin, capsule, and proteases have been demonstrated to cause attenuated virulence. Furthermore, both capsule and melanin production are regulated via a heterotrimeric G protein that requires GTP to function and, by extension, are dependent on the synthesis of GTP themselves (69).

Given the auxotrophy and lag observed in the production of virulence factors, we investigated the importance of *GUA1* during infection. Both the nematode and murine models of infection showed that *GUA1* is essential for virulence, mirroring the reports for *C. albicans* and *A. fumigatus* (26, 44). Furthermore, in the murine inhalation model, the *gua1*Δ strain was completely cleared by the host immune system.

Together, the *in vitro* phenotypic assays and the *in vivo* virulence models show that GMP synthase could be an useful drug target. Beyond the obvious requirements for GTP in DNA synthesis, transcription, and energy metabolism, many cellular processes are dependent on regulation via GTP-binding proteins. Furthermore, the production of the characteristic capsule of *C. neoformans*, the pathogen's most well known virulence factor, requires GDP-mannose for its biosynthesis (70). Inhibition of GMP synthase would prevent these key biological processes and thus be even more detrimental to *C. neoformans* survival in the hostile host environment.

The biochemistry and the structure of GMP synthase is key information that could enable the exploitation of this enzyme as an antifungal drug target, helping address the urgent need for novel chemotherapeutic agents to combat disseminated mycoses. GMP synthase consists of two active sites: one for the binding of glutamine and the other for XMP and ATP. The homology model and sequence alignment of *C. neoformans* GMP synthase to the human enzyme shows that the catalytic triad required for glutamine binding is conserved, although kinetic data show *C. neoformans* GMP synthase protein to have a lower affinity for this substrate, maybe because of other residues hindering binding. The best known inhibitor of GMP synthase in other species is DON, a well characterized glutamine agonist that targets several glutamine binding proteins. However, given the lower affinity of the *C. neoformans* GMP synthase protein for glutamine as a substrate, it is likely an unsuitable target for DON-based inhibition and additionally be a nonspecific target (65–67). In contrast, XMP amination requires interactions with eight residues in human GMP synthase, of which only five are homologous to the *C. neoformans* enzyme. The fact that the human GMP synthase residue Gln^{610} is not present in its fungal homolog, along with residues around the XMP binding site, may make targeting this site in antifungal development worthwhile.

The structural differences between GMP synthase in humans and *C. neoformans* identified via homology modeling are consistent with this difference potentially arising from marked changes in the dimerization domain that contributes key residues to the human XMP binding site as seen in the solved *E. coli* structure. These differences in the binding site of XMP may enable the development of selective compounds that do not interact with the human enzyme.

Limited insights into potential starting points for GMP synthase inhibitor development were provided in our study of ECC1385, which demonstrated potent activity against the purified *C. neoformans* GMP synthase but was unable to show activity in a whole cell assay. Rodriguez-Suarez *et al.* (26) demonstrated whole cell activity against *C. albicans in vitro* but not *in vivo*, instead finding that increased concentrations lead to toxicity in the murine model. ECC1385 has specificity toward GMP synthase; however, it is not adequately active toward fungi. This could simply be due to an inability to enter the cell.

The mechanism of action of GMP synthase requires all bound substrates to undergo an intermediate reaction before coming together to form GMP (34). How this secondary reaction (whereby the adenyl-XMP and GATase domain product are brought together) occurs is largely unknown, because the catalytic domains are ~30 Å apart in the available crystal structures. To enable GMP synthesis to occur, the enzyme must either channel the intermediates or undergo a large conformational change whereby both domains are brought together (34). It has been suggested that this large conformational change could be facilitated by the presence of XMP, ATP and Mg^{2+}. When the substrates are bound, the structure likely transitions into a compact state, creating an ammonia channel that enables the product of the GATase domain to react with adenyl-XMP (34, 36). The ability to undergo such a large conformational change may have contributed to our inability to acquire high quality diffraction data from our crystallization efforts.

Overall, we have demonstrated that GMP synthase is crucial for virulence factor production and pathogenesis of *C. neoformans* in both murine and nematode models. Differences between human and *C. neoformans* in enzymatic activity and amino acids of the XMP binding site make GMP synthase an attractive antifungal drug target. Historically, the *de novo* purine biosynthesis pathway has been a target for many drugs, in particular against cancer, because they are able to selectively target the demands of rapidly proliferating cells by starving them of essential nucleotides. Similarly, disseminating microbes rapidly proliferate during infection, making this an attractive target for antibiotics. Given the lack of current drugs on the market against fungi, novel targets like GMP synthase are urgently needed.

Experimental Procedures

Bioinformatic Analyses—The *C. neoformans* type strain H99 genome sequence was reported by Janbon *et al.* (47). The GMP synthase-encoding gene was identified in the *C. neoformans* genome via reciprocal best hit BLAST analysis querying with the *S. cerevisiae* Gua1 protein.

Strains and Medium—*C. neoformans* strains were cultured in liquid (1% yeast extract, 2% bacto-peptone, 2% glucose) or solid (additional 2% agar) YPD medium at 30 °C, and maintained at 4 °C for no longer than 2 weeks. *gua1*Δ mutants were cultured in liquid YNB (Becton Dickinson) medium supplemented with 2% glucose, 10 mM ammonium sulfate, and 1 mM guanine at 30 °C and maintained at 4 °C on solid YNB (additional 2% agar) supplemented as before unless otherwise stated. Cloning and plasmid preparation was performed in *E. coli* strain Mach1 (Life Technologies) cultured at 37 °C in lysogeny broth (LB; 1% tryptone, 0.5% yeast extract, 1% sodium chloride) supplemented with antibiotics as indicated and maintained on solid LB (2% agar) supplemented with antibiotics. For virulence assays, N2 Bristol *C. elegans* was maintained at 20 °C on NGM (48) seeded with *E. coli* strain OP50. Nematode virulence assays were subsequently performed on BHI medium (Becton Dickinson), NGM (48), or NGM supplemented with 1 mM guanine.

Molecular Techniques—The sequences of oligonucleotides used are listed in supplemental Table S1. The deletion construct for the *GUA1* gene was generated using overlap PCR, employing primers UQ1736 and UQ1739 to join the *GUA1* 5′ region (primers UQ1736 and UQ1737), the G418 resistance marker *NEO* (primers UQ234 and UQ235), and the *GUA1* 3′ region (primers UQ1738 and UQ1739). H99 genomic DNA was used as the template for *GUA1*, and the plasmid pJAF1 was used for *NEO* (49). The deletion construct was transformed into type strain H99 via biolistic transformation with a Bio-Rad He-1000 Biolistic device (Bio-Rad) with selection on medium containing 100 μg/ml G418 and 1 mM guanine. For complementation, the *GUA1* gene was PCR-amplified (primers UQ1736 and UQ1739) from H99 genomic DNA, digested with SpeI and XhoI and cloned into the nourseothricin resistance vector pCH233 cut with SpeI/XhoI to generate pAK05. The pAK05 *GUA1 NAT* fragment was subsequently purified as a 6167-bp SpeI/FspI fragment and transformed into the *gua1*Δ mutant,

selecting for nourseothricin resistance (100 μg/ml). For strain validation, genomic DNA was prepared using the CTAB protocol of Pitkin *et al.* (50), digested, electrophoresed on TAE-agarose gels, and Southern-blotted onto Hybond-XL membrane (GE Healthcare, UK) using standard procedures (51). Probes (primers UQ1736 and UQ1739) were generated using the Rediprime II kit and [α-^{32}P]dCTP (PerkinElmer Life Sciences). The blots were hybridized at 65 °C, and the membranes were exposed onto Fuji Super RX medical X-ray film (Fujifilm).

Phenotypic Assays—Production of melanin was assayed on L-DOPA medium (52) supplemented with 1 mM guanine. Urease assays were performed on Christensen's agar (53), and protease assays were performed on YNB with amino acids and ammonium sulfate supplemented with 2% glucose, 0.1% BSA, and 1 mM guanine. Images were collected after 24–92 h at 30 or 37 °C. All growth tests were performed in triplicate.

For capsule assays, strains were incubated in RPMI 1640 medium (Life Technologies) supplemented with 2% glucose, 10% fetal bovine serum (Life Technologies), and 1 mM guanine with shaking at 30 or 37 °C. At 30 h, cells were collected and stained with India ink (Becton Dickinson) and imaged with a Leica DM2500 microscope and DFC425C camera. At least 10 independent images were taken, and the relative capsule diameter of 50 cells from each culture was determined as described by Zaragoza *et al.* (54). Experiments were performed in biological triplicate, and analysis of variance tests were performed in GraphPad Prism version 7.0 (GraphPad Software) to compare variation between replicates.

Growth curves were conducted in RPMI 1640 medium supplemented with 2% glucose, 10% fetal bovine serum, and 1 mM guanine at 30 °C. Starter cultures were grown overnight, diluted to A_{600} 0.05, and then monitored spectrophotometrically at A_{600} every 12 h for 6 days. Growth curves were performed in triplicate.

Nematode Virulence Assays—H99, *gua1*Δ, and *gua1*Δ+*GUA1* strains were grown at 30 °C overnight on BHI, minimal medium, and minimal medium supplemented with 1 mM guanine prior to the introduction of 30–50 synchronized young adult *C. elegans* worms and incubation at 28 °C. Worms were counted every 24 h for 8 days; individuals that did not respond to touch with a platinum wire pick were considered dead and removed. Experimental conditions were tested in triplicate, with Kaplan-Meier survival curves and Mantel-Cox tests performed in GraphPad Prism version 7.0 (GraphPad Software) to determine significance.

Murine Inhalation Model of Cryptococcosis—For murine infection assays, 6-week-old female BALB/c mice (Animal Resources Centre, Murdoch, Australia) were infected by nasal inhalation (55). For each strain, 10 mice were inoculated with a 50-μl drop containing 5×10^5 *C. neoformans* cells. A maximum of five mice were housed per individually ventilated cage (Tecniplast) with Bed-o'Cobs 1/8-inch bedding (Andersons), Crink-l'Nest nesting material (Andersons), and cardboard as environmental enrichment. The mice were provided rat and mouse cubes (Specialty Feeds, Glen Forrest, Australia) and water *ad libitum*. Each mouse was examined and weighed twice daily for the duration of the experiment, with affected mice euthanized via CO_2 inhalation once body weight had decreased to 80% of preinfection weight or they exhibited symptoms consistent with infection. Death after CO_2 inhalation was confirmed by pedal reflex prior to dissection. Brain, lungs, liver, spleen, and kidneys were collected, homogenized in 1 ml of PBS using a TissueLyser II (Qiagen), serially diluted, and plated on YPD supplemented with 100 μg/ml ampicillin, 50 μg/ml kanamycin, and 25 μg/ml chloramphenicol (H99 and *gua1*Δ+*GUA1* infected mice) or YNB supplemented with 1 mM guanine and antibiotics as before (*gua1*Δ infected mice). The plates were incubated at 30 °C, and after 2 days colonies were counted and used to calculate colony-forming units/g of organ. Kaplan-Meier survival curves were plotted using GraphPad Prism version 7.0 (GraphPad Software). Significance was analyzed using the log-rank test, whereas organ burden significance was determined using a one-way analysis of variance with Tukey's multiple comparisons test. p values of < 0.05 were considered significant.

Ethics Statement—This study was carried out in strict accordance with the recommendations in the Australian Code of Practice for the Care and Use of Animals for Scientific Purposes by the National Health and Medical Research Council. The protocol was approved by the Molecular Biosciences Animal Ethics Committee of the University of Queensland (approval number SCMB/008/11/UQ/NHMRC). Infection was performed under methoxyflurane anesthesia, and all efforts were made to minimize suffering through adherence to the Guidelines to Promote the Wellbeing of Animals Used for Scientific Purposes as put forward by the National Health and Medical Research Council.

Broth Microdilution Assays—Minimum inhibitory concentration susceptibility of *C. neoformans* to ECC1385 was determined in accordance with the CLSI M27-A2 guidelines, with the following modifications: YNB medium supplemented with ammonium sulfate and 2% glucose, final inoculum concentration of $1.5–2.0 \times 10^3$ cells/ml and incubation at 35 °C for 72 h (25, 56). Drug concentrations ranged from 100 μM to 49 nM; the MIC was defined as the concentration that prevented any discernible growth after 72 h. Fluconazole was employed as a control.

Expression and Purification of C. neoformans GMP Synthase—Total RNA was isolated from strain H99 using TRIzol reagent (Invitrogen), with intron-free cDNA and then synthesized using a Bioline cDNA synthesis kit (Bioline). The *GUA1* ORF was subsequently PCR-amplified (primers UQ2081 and UQ2082), and the product was inserted via ligation-independent cloning into the SspI site of His tag vector pMCSG7 (57) to yield pJLC1 and then co-transformed with pLysS into *E. coli* strain BL21(DE3) (Merck). Transformed cells were grown at 37 °C in LB supplemented with 100 mg/ml ampicillin and 12.5 mg/ml chloramphenicol to an A_{600} of ~1 then induced with 1 mM isopropyl β-D-1-thiogalactopyranoside and grown for a further 17 h at 22 °C. The cells were harvested and resuspended in lysis buffer (50 mM HEPES, pH 8.0, 300 mM NaCl, 30 mM imidazole, 1 mM DTT, and 1 mM PMSF) before disruption with a Sonifier W-450 Digital Ultrasonic Cell Disruptor sonicator (Branson). Following centrifugation, supernatant was loaded onto a 5-ml HisTrap Fast Flow column (GE Healthcare) to purify the histidine tagged protein by immobilized nickel affin-

ity chromatography. The protein was eluted in a linear gradient of 30–500 mM imidazole, with a single elution peak. Peak fractions were pooled, concentrated, and incubated overnight with 500 μg of tobacco etch virus protease at 4 °C to cleave the N-terminal histidine tag. Following a second round of nickel affinity chromatography, GMP synthase was collected from the flowthrough, concentrated, and further purified using a HiLoad 26/600 Superdex 200 SEC column (GE Healthcare). Protein was eluted at a rate of 2.5 ml/min with SEC buffer (10 mM HEPES, pH 7.5, 150 mM NaCl, and 1 mM DTT) using an ÄKTA-purifier FPLC system (GE Healthcare). Peak fractions were combined and concentrated to ~32 mg/ml and flash frozen in liquid nitrogen for storage at −80 °C.

Steady-state and Inhibitor Kinetics—GMP synthase activity was monitored spectrophotometrically using a Cary60 UV-visible spectrophotometer (Agilent). Assays were carried out as described for *M. tuberculosis* by Franco *et al.* (58) with the exception of 50 mM HEPES, pH 7.5, being used instead of 50 mM Tris, pH 7.5; optimized reaction conditions were determined as 0.15 mM XMP, 1 mM ATP, 5 mM glutamine, and 20 mM $MgCl_2$. The temperature used was 40 °C, consistent with previous assays conducted for the human, *E. coli*, and *M. tuberculosis* enzymes; this temperature also gave the highest activity in *C. neoformans* GMP synthase (35, 58, 59). Purified *C. neoformans* GMP synthase was used at 0.025 mg/ml final concentration in the assay. Assays were performed in triplicate by measuring the decrease of absorbance at 290 nm to follow conversion of XMP (ϵ_{290} = 4.080 mM^{-1} cm^{-1}) into GMP (ϵ_{290} = 3.066 mM^{-1} cm^{-1}). $\Delta\epsilon$ = 1.014 mM^{-1} cm^{-1} was used to calculate the amount of GMP formed. The data were fitted to the Hill or Michaelis-Menten equations using GraphPad Prism version 7.0 (GraphPad Software) as appropriate (Figure S1). The Hill equation was used to calculate the Hill coefficient (n) (Equation 1) (60). IC_{50} values were determined using standard assay conditions with varying concentrations of inhibitor ECC1385 (0–100 μM) (Figure S2).

$$v = \frac{V_{max}[S]^n}{{K_{0.5}}^n + [S]^n} \quad \text{(Eq. 1)}$$

Multiangle Laser Light Scattering—SEC coupled with MALLS was performed using a Dawn Heleos II 18 angle light-scattering detector coupled with an Optilab rEX refractive index detector (Wyatt Technology). 500 μg of GMP synthase was applied to the HiLoad 26/600 Superdex 200 SEC column at a flow rate of 0.5 ml/min in 10 mM HEPES, pH 7.5, 150 mM NaCl, and 1 mM DTT. Molecular mass calculations were performed using Astra 5.3 software (Wyatt Technology). Input of the refractive increment (dn/dc values) was set at 0.186 in molecular mass calculations (61).

Crystallization Screens and Modeling of GMP Synthase—Crystallization experiments of recombinant *C. neoformans* GMP synthase were performed by hanging drop vapor diffusion at 20 °C with the commercial sparse matrix screens JCSG, Morpheus, PACT, ProPlex (Molecular Dimensions), INDEX, PEG/Ion and PEGRx (Hampton Research). Two initial lead conditions (PACT F8, 20% PEG 3350, 0.2 M sodium sulfate decahydrate, and 0.1 M Bis-Tris propane, pH 6.5, and PACT G8, 20% PEG 3350, 0.2 M sodium sulfate decahydrate, and 0.1 M Bis-Tris propane, pH 7.5) were chosen for factorial grid screen optimization. Despite significant efforts—co-crystallization with substrates (XMP, AMP-PNP, and $MgCl_2$), streak and microseeding, enhanced nucleation (62), Silver Bullets (Hampton Research), and Additive Screen (Molecular Dimension)—the best resolution diffraction results that could be achieved using the MX2 beamline at the Australian Synchrotron was 6 Å. Subsequently we utilized homology modeling of *C. neoformans* GMP synthase using the automated webserver Modeler (63) with the *E. coli* GMP synthase (50% protein identity) structure as a template (PDB code 1GPM) (34).

Author Contributions—J. L. C., T. L. T., B. K., S. J. W., U. K., and J. A. F. conceived and designed the experiments. J. L. C., T. L. T., S. J. W., Y. Q. A. E. K., E. C. C., and A. A. B. R. performed the experiments. J. L. C., T. L. T., S. J. W., B. K., U. K., and J. A. F. analyzed the data. J. C. and J. A. F. wrote the paper. S. J. W., M. S. B., A. A. B. R., M. A. C., and B. K. contributed to editing and writing.

Acknowledgments—We acknowledge use of the University of Queensland Remote Operation Crystallization and X-ray Diffraction Facility. We thank Terry Roemer at Merck for supplying ECC1385.

References

1. GBD 2015 HIV Collaborators (2016) Estimates of global, regional, and national incidence, prevalence, and mortality of HIV, 1980–2015: the Global Burden of Disease Study 2015. *Lancet HIV* **3,** e408
2. Hymes, K. B., Cheung, T., Greene, J. B., Prose, N. S., Marcus, A., Ballard, H., William, D. C., and Laubenstein, L. J. (1981) Kaposi's sarcoma in homosexual men: a report of eight cases. *Lancet* **2,** 598–600
3. Centers for Disease Control (CDC) (1981) Kaposi's sarcoma and *Pneumocystis* pneumonia among homosexual men: New York City and California. *MMWR Morb. Mortal. Wkly. Rep.* **30,** 305–308
4. Centers for Disease Control (CDC) (1982) Update on acquired immune deficiency syndrome (AIDS): United States. *MMWR Morb. Mortal. Wkly. Rep.* **31,** 507–508, 513–514
5. Centers for Disease Control (CDC) (1983) Update: acquired immunodeficiency syndrome (AIDS): United States. *MMWR Morb. Mortal Wkly. Rep.* **32,** 465–467
6. Marx, J. L. (1984) Strong new candidate for AIDS agent. *Science* **224,** 475–477
7. Roberts, B. D. (1994) HIV antibody testing methods: 1985–1988. *J. Insur. Med.* **26,** 13–14
8. Yarchoan, R., Klecker, R. W., Weinhold, K. J., Markham, P. D., Lyerly, H. K., Durack, D. T., Gelmann, E., Lehrman, S. N., Blum, R. M., Barry, D. W., *et al.* (1986) Administration of 3′-azido-3′-deoxythymidine, an inhibitor of HTLV-III/LAV replication, to patients with AIDS or AIDS-related complex. *Lancet* **1,** 575–580
9. Riesenberg, D. E., and Marwick, C. (1985) Anti-AIDS agents show varying early results *in vitro* and *in vivo*. *JAMA* **254,** 2521, 2527, 2529
10. WHO (2016) Global Health Observatory (GHO) data, http://www.who.int/gho/hiv/en/ (accessed August 23, 2016)
11. Perfect, J. R. (2014) Cryptococcosis: a model for the understanding of infectious diseases. *J. Clin. Invest.* **124,** 1893–1895
12. Bicanic, T., Harrison, T., Niepieklo, A., Dyakopu, N., and Meintjes, G. (2006) Symptomatic relapse of HIV-associated cryptococcal meningitis after initial fluconazole monotherapy: the role of fluconazole resistance and immune reconstitution. *Clin. Infect. Dis.* **43,** 1069–1073
13. Jongwutiwes, U., Sungkanuparph, S., and Kiertiburanakul, S. (2008) Comparison of clinical features and survival between cryptococcosis in human immunodeficiency virus (HIV)-positive and HIV-negative patients. *Jpn. J. Infect. Dis.* **61,** 111–115

14. Li, M., Liao, Y., Chen, M., Pan, W., and Weng, L. (2012) Antifungal susceptibilities of Cryptococcus species complex isolates from AIDS and non-AIDS patients in Southeast China. *Braz. J. Infect. Dis.* **16,** 175–179
15. Vermes, A., Guchelaar, H. J., and Dankert, J. (2000) Flucytosine: a review of its pharmacology, clinical indications, pharmacokinetics, toxicity and drug interactions. *J. Antimicrob. Chemother.* **46,** 171–179
16. WHO (2011) Rapid Advice: Diagnosis, Prevention and Management of Cryptococcal Disease in HIV-infected Adults, Adolescents and Children. World Health Organisation, Geneva, Switzerland
17. Elion, G. B. (1989) Nobel lecture: The purine path to chemotherapy. *Biosci. Rep.* **9,** 509–529
18. Elion, G. B. (1985) An overview of the role of nucleosides in chemotherapy. *Adv. Enzyme Regul.* **24,** 323–334
19. Hitchings, G. H., Elion, G. B., and Vanderwerff, H. (1948) 2-Aminopurine as a purine antagonist. *Fed. Proc.* **7,** 160
20. Christopherson, R. I., Lyons, S. D., and Wilson, P. K. (2002) Inhibitors of *de novo* nucleotide biosynthesis as drugs. *Acc. Chem. Res.* **35,** 961–971
21. Skipper, H. E., Thomson, J. R., Elion, G. B., and Hitchings, G. H. (1954) Observations on the anticancer activity of 6-mercaptopurine. *Cancer Res.* **14,** 294–298
22. Mendelsohn, L. G., Shih, C., Schultz, R. M., and Worzalla, J. F. (1996) Biochemistry and pharmacology of glycinamide ribonucleotide formyltransferase inhibitors: LY309887 and lometrexol. *Invest. New Drugs* **14,** 287–294
23. Franklin, T. J., and Cook, J. M. (1969) The inhibition of nucleic acid synthesis by mycophenolic acid. *Biochem. J.* **113,** 515–524
24. Sweeney, M. J., Hoffman, D. H., and Esterman, M. A. (1972) Metabolism and biochemistry of mycophenolic acid. *Cancer Res.* **32,** 1803–1809
25. Morrow, C. A., Valkov, E., Stamp, A., Chow, E. W., Lee, I. R., Wronski, A., Williams, S. J., Hill, J. M., Djordjevic, J. T., Kappler, U., Kobe, B., and Fraser, J. A. (2012) *De novo* GTP biosynthesis is critical for virulence of the fungal pathogen *Cryptococcus neoformans*. *PLoS Pathogens* **8,** e1002957
26. Rodriguez-Suarez, R., Xu, D., Veillette, K., Davison, J., Sillaots, S., Kauffman, S., Hu, W., Bowman, J., Martel, N., Trosok, S., Wang, H., Zhang, L., Huang, L. Y., Li, Y., Rahkhoodaee, F., *et al.* (2007) Mechanism-of-action determination of GMP synthase inhibitors and target validation in *Candida albicans* and *Aspergillus fumigatus*. *Chem. Biol.* **14,** 1163–1175
27. Blundell, R. D., Williams, S. J., Arras, S. D., Chitty, J. L., Blake, K. L., Ericsson, D. J., Tibrewal, N., Rohr, J., Koh, Y. Q., Kappler, U., Robertson, A. A., Butler, M. S., Cooper, M. A., Kobe, B., and Fraser, J. A. (2016) Disruption of *de novo* adenosine triphosphate (ATP) biosynthesis abolishes virulence in *Cryptococcus neoformans*. *ACS Infect. Dis.* **2,** 651–663
28. Eells, J. T., and Spector, R. (1983) Purine and pyrimidine base and nucleoside concentrations in human cerebrospinal fluid and plasma. *Neurochem. Res.* **8,** 1451–1457
29. Rodríguez-Núñez, A., Camiña, F., Lojo, S., Rodríguez-Segade, S., and Castro-Gago, M. (1993) Concentrations of nucleotides, nucleosides, purine bases and urate in cerebrospinal fluid of children with meningitis. *Acta Paediatr.* **82,** 849–852
30. Kuračka, L., Kalnovičová, T., Kucharská, J., and Turčáni, P. (2014) Multiple sclerosis: evaluation of purine nucleotide metabolism in central nervous system in association with serum levels of selected fat-soluble antioxidants. *Mult. Scler. Int.* **2014,** 759808
31. Abrams, R., and Bentley, M. (1955) Biosynthesis of nucleic acid purines: I. Formation of guanine from adenine compounds in bone marrow extracts. *Arch. Biochem. Biophys.* **56,** 184–195
32. Lagerkvist, U. (1958) Biosynthesis of guanosine 5′-phosphate: II. Amination of xanthosine 5′-phosphate by purified enzyme from pigeon liver. *J. Biol. Chem.* **233,** 143–149
33. Fukuyama, T. T. (1966) Formation of an adenyl xanthosine monophosphate intermediate by xanthosine 5′-phosphate aminase and its inhibition by psicofuranine. *J. Biol. Chem.* **241,** 4745–4749
34. Tesmer, J. J., Klem, T. J., Deras, M. L., Davisson, V. J., and Smith, J. L. (1996) The crystal structure of GMP synthetase reveals a novel catalytic triad and is a structural paradigm for two enzyme families. *Nat. Struct. Biol.* **3,** 74–86
35. Abbott, J. L., Newell, J. M., Lightcap, C. M., Olanich, M. E., Loughlin, D. T., Weller, M. A., Lam, G., Pollack, S., and Patton, W. A. (2006) The effects of removing the GAT domain from E. coli GMP synthetase. *Protein J.* **25,** 483–491
36. Oliver, J. C., Linger, R. S., Chittur, S. V., and Davisson, V. J. (2013) Substrate activation and conformational dynamics of guanosine 5′-monophosphate synthetase. *Biochemistry* **52,** 5225–5235
37. Oliver, J. C., Gudihal, R., Burgner, J. W., Pedley, A. M., Zwierko, A. T., Davisson, V. J., and Linger, R. S. (2014) Conformational changes involving ammonia tunnel formation and allosteric control in GMP synthetase. *Arch. Biochem. Biophys.* **545,** 22–32
38. von der Saal, W., Crysler, C. S., and Villafranca, J. J. (1985) Positional isotope exchange and kinetic experiments with *Escherichia coli* guanosine-5′-monophosphate synthetase. *Biochemistry* **24,** 5343–5350
39. Lee, B. H., and Hartman, S. C. (1974) Preferential utilization of glutamine for amination of xanthosine 5′-phosphate to guanosine 5′-phosphate by purified enzymes from *Escherichia coli*. *Biochem. Biophys. Res. Commun.* **60,** 918–925
40. Franklin, M. C., Cheung, J., Rudolph, M. J., Burshteyn, F., Cassidy, M., Gary, E., Hillerich, B., Yao, Z. K., Carlier, P. R., Totrov, M., and Love, J. D. (2015) Structural genomics for drug design against the pathogen *Coxiella burnetii*. *Proteins* **83,** 2124–2136
41. Maruoka, S., Horita, S., Lee, W. C., Nagata, K., and Tanokura, M. (2010) Crystal structure of the ATPPase subunit and its substrate-dependent association with the GATase subunit: a novel regulatory mechanism for a two-subunit-type GMP synthetase from *Pyrococcus horikoshii* OT3. *J. Mol. Biol.* **395,** 417–429
42. Ballut, L., Violot, S., Shivakumaraswamy, S., Thota, L. P., Sathya, M., Kunala, J., Dijkstra, B. W., Terreux, R., Haser, R., Balaram, H., and Aghajari, N. (2015) Active site coupling in *Plasmodium falciparum* GMP synthetase is triggered by domain rotation. *Nat. Commun.* **6,** 8930
43. Welin, M., Lehtiö, L., Johansson, A., Flodin, S., Nyman, T., Trésaugues, L., Hammarström, M., Gräslund, S., and Nordlund, P. (2013) Substrate specificity and oligomerization of human GMP synthetase. *J. Mol. Biol.* **425,** 4323–4333
44. Jiang, L., Zhao, J., Guo, R., Li, J., Yu, L., and Xu, D. (2010) Functional characterization and virulence study of ADE8 and GUA1 genes involved in the *de novo* purine biosynthesis in *Candida albicans*. *FEMS Yeast Res.* **10,** 199–208
45. Gardner, W. J., and Woods, R. A. (1979) Isolation and characterisation of guanine auxotrophs in *Saccharomyces cerevisiae*. *Can. J. Microbiol.* **25,** 380–389
46. Dujardin, G., Kermorgant, M., Slonimski, P. P., and Boucherie, H. (1994) Cloning and sequencing of the GMP synthetase-encoding gene of *Saccharomyces cerevisiae*. *Gene* **139,** 127–132
47. Janbon, G., Ormerod, K. L., Paulet, D., Byrnes, E. J., 3rd, Yadav, V., Chatterjee, G., Mullapudi, N., Hon, C. C., Billmyre, R. B., Brunel, F., Bahn, Y. S., Chen, W., Chen, Y., Chow, E. W., Coppée, J. Y., *et al.* (2014) Analysis of the genome and transcriptome of *Cryptococcus neoformans* var. grubii reveals complex RNA expression and microevolution leading to virulence attenuation. *PLoS Genet.* **10,** e1004261
48. Brenner, S. (1974) The genetics of *Caenorhabditis elegans*. *Genetics* **77,** 71–94
49. Fraser, J. A., Subaran, R. L., Nichols, C. B., and Heitman, J. (2003) Recapitulation of the sexual cycle of the primary fungal pathogen *Cryptococcus neoformans* var. gattii: implications for an outbreak on Vancouver Island, Canada. *Eukaryotic Cell* **2,** 1036–1045
50. Pitkin, J. W., Panaccione, D. G., and Walton, J. D. (1996) A putative cyclic peptide efflux pump encoded by the TOXA gene of the plant-pathogenic fungus *Cochliobolus carbonum*. *Microbiology* **142,** 1557–1565
51. Sambrook, J. F., and Maniatis, T. (1989) *Molecular Cloning: A Laboratory Manual*, 2nd ed., Cold Spring Harbor Laboratory Press, Cold Spring Harbor, NY
52. Chaskes, S., and Tyndall, R. L. (1975) Pigment production by *Cryptococcus neoformans* from para- and ortho-diphenols: effect of the nitrogen source. *J. Clin. Microbiol.* **1,** 509–514
53. Christensen, W. B. (1946) Urea decomposition as a means of differentiating proteus and paracolon cultures from each other and from *Salmonella* and *Shigella* types. *J. Bacteriol.* **52,** 461–466

54. Zaragoza, O., Fries, B. C., and Casadevall, A. (2003) Induction of capsule growth in *Cryptococcus neoformans* by mammalian serum and CO_2. *Infect. Immun.* **71,** 6155–6164
55. Cox, G. M., Mukherjee, J., Cole, G. T., Casadevall, A., and Perfect, J. R. (2000) Urease as a virulence factor in experimental cryptococcosis. *Infect. Immun.* **68,** 443–448
56. Ghannoum, M. A., and Rice, L. B. (1999) Antifungal agents: mode of action, mechanisms of resistance, and correlation of these mechanisms with bacterial resistance. *Clin. Microbiol. Rev.* **12,** 501–517
57. Stols, L., Gu, M., Dieckman, L., Raffen, R., Collart, F. R., and Donnelly, M. I. (2002) A new vector for high-throughput, ligation-independent cloning encoding a tobacco etch virus protease cleavage site. *Protein Expr. Purif.* **25,** 8–15
58. Franco, T. M., Rostirolla, D. C., Ducati, R. G., Lorenzini, D. M., Basso, L. A., and Santos, D. S. (2012) Biochemical characterization of recombinant guaA-encoded guanosine monophosphate synthetase (EC 6.3.5.2) from *Mycobacterium tuberculosis* H37Rv strain. *Arch. Biochem. Biophys.* **517,** 1–11
59. Nakamura, J., and Lou, L. (1995) Biochemical characterization of human GMP synthetase. *J. Biol. Chem.* **270,** 7347–7353
60. Hill, A. V. (1910) The possible effects of the aggregation of the molecules of hemoglobin on its dissociation curves. *J. Physiol.* **40,** 4–7
61. Wen, J., Arakawa, T., and Philo, J. S. (1996) Size-exclusion chromatography with on-line light-scattering, absorbance, and refractive index detectors for studying proteins and their interactions. *Anal. Biochem.* **240,** 155–166
62. Thakur, A. S., Robin, G., Guncar, G., Saunders, N. F., Newman, J., Martin, J. L., and Kobe, B. (2007) Improved success of sparse matrix protein crystallization screening with heterogeneous nucleating agents. *PLoS One* **2,** e1091
63. Sali, A., and Blundell, T. L. (1993) Comparative protein modelling by satisfaction of spatial restraints. *J. Mol. Biol.* **234,** 779–815
64. Mylonakis, E., Ausubel, F. M., Perfect, J. R., Heitman, J., and Calderwood, S. B. (2002) Killing of *Caenorhabditis elegans* by *Cryptococcus neoformans* as a model of yeast pathogenesis. *Proc. Natl. Acad. Sci. U.S.A.* **99,** 15675–15680
65. Rahman, A., Smith, F. P., Luc, P. T., and Woolley, P. V. (1985) Phase I study and clinical pharmacology of 6-diazo-5-oxo-L-norleucine (DON). *Invest. New Drugs* **3,** 369–374
66. Cervantes-Madrid, D., Romero, Y., and Dueñas-González, A. (2015) Reviving lonidamine and 6-diazo-5-oxo-L-norleucine to be used in combination for metabolic cancer therapy. *BioMed Res. Int.* **2015,** 690492
67. Coggin, J. H., Jr., and Martin, W. R. (1965) 6-Diazo-5-oxo-L-norleucine inhibition of *Escherichia coli*. *J. Bacteriol.* **89,** 1348–1353
68. Sakamoto, N., Hatfield, G. W., and Moyed, H. S. (1972) Physical properties and subunit structure of xanthosine 5′-phosphate aminase. *J. Biol. Chem.* **247,** 5880–5887
69. Alspaugh, J. A., Perfect, J. R., and Heitman, J. (1997) *Cryptococcus neoformans* mating and virulence are regulated by the G-protein alpha subunit GPA1 and cAMP. *Genes Dev.* **11,** 3206–3217
70. Zaragoza, O., Rodrigues, M. L., De Jesus, M., Frases, S., Dadachova, E., and Casadevall, A. (2009) The capsule of the fungal pathogen *Cryptococcus neoformans*. *Adv. Appl. Microbiol.* **68,** 133–216
71. Bhat, J. Y., Shastri, B. G., and Balaram, H. (2008) Kinetic and biochemical characterization of *Plasmodium falciparum* GMP synthetase. *Biochem. J.* **409,** 263–273
72. Robert, X., and Gouet, P. (2014) Deciphering key features in protein structures with the new ENDscript server. *Nucleic Acids Res.* **42,** W320–W324

GMP Synthase Is Required for Virulence Factor Production and Infection by *Cryptococcus neoformans*

Jessica L. Chitty, Tayla L. Tatzenko, Simon J. Williams, Y. Q. Andre E. Koh, Elizabeth C. Corfield, Mark S. Butler, Avril A. B. Robertson, Matthew A. Cooper, Ulrike Kappler, Bostjan Kobe and James A. Fraser

J. Biol. Chem. 2017, 292:3049-3059.
doi: 10.1074/jbc.M116.767533 originally published online January 6, 2017